Suspension characteristics and electrophoretic deposition ofp-Type Bi2Te3Films for thermoelectric applications

TALEBI, Tahereh, GHOMASHCHI, Reza, TALEMI, Pejman and AMINORROAYA YAMINI, Sima <http://orcid.org/0000-0002-2312-8272>

Suspension characteristics and electrophoretic deposition of *p*-type Bi_2Te_3 films for thermoelectric applications

Tahereh Talebi[*1], Reza Ghomashchi[2], Pejman Talemi[3], Sima Aminorroaya[4]

1. The School of Mechanical Engineering, The University of Adelaide, South Australia, Australia. tahereh.talebinamakrodbari@adelaide.edu.au.
2. The School of Mechanical Engineering, The University of Adelaide, South Australia, Australia. reza.ghomashchi@adelaide.edu.au
3. The School of Chemical Engineering, The University of Adelaide, South Australia, Australia. pejman.talemi@adelaide.edu.au
4. Sheffield Hallam University, Sheffield, England. S.Aminorroaya-Yamini@shu.ac.uk

Abstract

Electrophoretic deposition (EPD) was utilized to prepare uniform crack-free Bi_2Te_3 films for thermoelectric applications, effectively. A *p*-type Bi_2Te_3 film with a coherent structure and even thickness, was deposited from Tetrahydrofuran (THF) suspensions and examined using a scanning electron microscope (SEM). The specific weights of the depositions, the effective percentile coverage of the films on the substrate, the zeta potential and the electrical conductivity of different suspensions and the in-plane Seebeck coefficients of the Bi_2Te_3 films were measured. Although the Seebeck coefficient value of the EPD film (126 μV/K) was approximately 25% lower than the highest value reported for Bi_2Te_3 in the open literature via the co-sputtering method (160 μV/K), one of the complex and expensive routes, the cost-effectiveness and the speed of the simple EPD process is an undeniable advantage. This could open up new opportunities for the application of films to commercialize thermoelectric generators (TEG). It is interesting to note that the value of the Seebeck coefficient for our EPD-fabricated film was higher than for some of the other types of coatings prepared by more expensive and sophisticated fabrication routes, such as for the electrodeposition technique (80 μV/K), for example.

[1] phone: +61883-133-360; fax: +61883-134-367

Keywords: Electrical conductivity; Electrophoretic deposition (EPD); Suspension; Bi_2Te_3 Films; Thermoelectric materials; Seebeck coefficient.

Introduction

One of the ways of dealing with the energy crisis is to increase the energy efficiency of our energy generating and consuming systems, such as electricity generating and heavy industry manufacturing plants, respectively [1], where a large portion of energy is lost in the form of waste heat. If the waste heat could be converted back into electricity, a new, enormous source of cheap, clean energy could boost society's prosperity, especially if the conversion does not cause problems for the environment. This is a feasible scenario if high performance thermoelectric generators (TEG) can be designed and fabricated. The efficiency of TEGs is heavily reliant on the development of more advanced thermoelectric materials for converting waste heat into electricity [2, 3].

TE materials are generally heavy and come at a high cost due to their lack of abundance. Therefore, the challenge is three-fold; lighter structures, more efficient TE (heat to electricity) conversion and cheaper TE materials and devices. In recent years, to overcome the high weight and cost of TE materials and increase their specific power, researchers have concentrated their attention on fabricating films made from TE materials, using different methods, and studying their particular TE properties [4-6]. Bi_2Te_3 is one of the most studied TE materials due to its high TE performance at room temperature [7].

Some of the methods explored for preparation of Bi_2Te_3 films include radio-frequency (RF) magnetron sputtering [8-12], electrodeposition [13], flash evaporating deposition [14], pulsed-electroplating [4, 15, 16], and even screen-printing and brush-printing [5, 17]. Each method has its

own unique advantages and disadvantages. For example, the co-sputtering method, which results in the deposition of Bi_2Te_3 films with the highest Seebeck coefficient (around 160-180μV/K) [12], is the most expensive method to apply and has a low deposition rate.

We have previously advocated the use of the electrophoretic deposition (EPD) method to fabricate uniform films of Bi_2Te_3 from colloidal suspensions, due to the low cost and high deposition rate [18, 19]. In the present work, various suspensions of Bi_2Te_3 powders were investigated in greater depth and with different parameters such as the zeta potential, the electrical conductivity of suspensions and the in-plane Seebeck coefficients, all of which were measured and discussed.

Under EPD, when a DC voltage is applied to charged powder particles suspended in a medium, the particles are attracted and deposited on the substrate with the opposite charge [20, 21].

Conventionally, EPD has been used to deposit wear-resistant and anti-oxidant ceramic coatings [20]. However, recently, functional films have been fabricated using EPD for various advanced applications such as microelectronic devices, solid oxide fuel cells, bioactive coatings, complex graded composites, gas diffusion electrodes and sensors, etc. [20, 22-25]. Thick films of various advanced and nanostructured materials such as silica [26], hydroxyapatite [27], nano-zeolite [28], carbon nanotubes [29], oxide nanorods [30], luminescent [31] and piezoelectric materials [32], and functionally graded ceramics [33] have also been fabricated using EPD.

The charge on the particle (the zeta potential) and its electrophoretic mobility in the suspension under the imposed electric field are the main driving forces of electrophoretic deposition [20, 21]. According to Hamaker's equation [34], the EPD deposit yield (w) is calculated through the following equation:

$$w = \int_{t_1}^{t_2} \mu . E . A . C . dt \quad (1)$$

where μ (cm/s) is the electrophoretic mobility; E (V) is the imposed electric field strength; A (m^2) is the surface area of the electrode; C (g/l) is the particle mass concentration and t (s) is the deposition time.

The electrophoretic mobility of particles (μ) is a critical property of the suspension and is given by [35]:

$$\mu = \frac{2}{3}\frac{\varepsilon_0 \varepsilon_r \zeta}{\eta} f(\kappa r) \quad (2)$$

where ε_0 (farad/meter) is the permittivity of the vacuum; ε_r is the relative permittivity of the solvent; ζ (V) is the zeta potential of the particles; η (cP) is the viscosity of the solvent; f(κr) is the Henry coefficient, which depends on the relationship between the thickness of the double layer ($1/\kappa$), (κ is the Debye-Huckel parameter) and the core radius (r) of the particle.

Although the above-mentioned parameters play an important role on the characteristics of the deposited EPD coating, the quality of the finished coating is influenced by other important factors such as the role of impurities [24, 36, 37], preparation and any aging of the suspension [38, 39], the environmental effects [40] as well as the role of electrode preparation [41, 42]. In addition, the results of specific materials dispersed in specific solvents and additives cannot be generalized to other materials, solvents or additives [43]. Therefore, in order to investigate the possibilities of EPD with a new material and discover its proper solvent-additive systems, one has to conduct a detailed analysis of the EPD process.

The characteristics of Bi_2Te_3 suspensions in terms of the EPD process have not yet been studied completely. The current article reports on a comprehensive study of the properties of Bi_2Te_3 suspensions, the specific weight of deposition, microstructure and TE properties (the Seebeck coefficient) of both green and sintered EPD deposited films.

Methodology

The details of the *p*-type Bi_2Te_3 ($Bi_{0.5}Se_{1.5}Te_3$) powder, which is commercially available with 99.99% purity, have been reported elsewhere [19]. The median particle size of powder (D50) was 10μm. A range of media (solvents) with 99.8% purities was acquired commercially.

The *p*-type Bi_2Te_3 suspensions were prepared by dispersing 1g of Bi_2Te_3 powder in 100 ml of the media mixture, using an ultrasonic bath for 15 minutes to break the agglomerates and stabilize the suspension. After 24 hours' rest for the suspensions to reach stability without any movements provided by external sources, an ultrasonic bath was again used for 2 minutes prior to the commencement of the EPD process. The list of various tested suspensions is given in Table 1.

The distance between the substrate and the counter electrode was constant at 10 mm for the EPD process. The electrodes were vertical and kept parallel during the EPD process (Figure 1). The substrate and the counter electrode were cut from a commercially obtained copper foil roll, with dimensions of 10mm by 10mm. The applied electric field was 100 V with a deposition time of 10 minutes. The sintering of the as-deposited (green) films was conducted in an Ar-controlled environment tube furnace at 693K for 1 hour. The optimizations of the EPD voltage and time were reported in our previous works [18, 19]. The optimum conditions for the sintering process, such as temperature and time, were determined through systematic investigation and the results will be reported in future publications.

The microstructures of the Bi_2Te_3 films have been characterized using SEM (a scanning electron microscope - Quanta 450) and the Rigaku MiniFlex 600 XRD was used to determine the changes in the phases and crystal structures of the green and sintered films. The chemical composition was measured using EDX (Energy-dispersive X-ray spectroscopy) of SEM. The Zeta potential of the particles was measured for all suspensions using a Malvern Zetasizer Nano Series. The electrical conductivity of the suspension was measured with a TPS WP-84

Conductivity-Salinity Meter device. To evaluate the thermoelectric properties of the deposited films, an MMR Seebeck Measurement System (SB1000-K2000) was used to measure the in-plane Seebeck coefficient of the films at 300K. The films were separated from the Cu substrate before measuring its Seebeck coefficients to eliminate the Cu substrate effect on the Seebeck coefficients of the deposited films. A large number of samples was prepared and the SEM, XRD, density and Seebeck coefficients measurement experiments were repeated at least 20 times on various samples. The reported data is an average amount.

TABLE 1. LIST OF SOME OF THE VARIOUS TESTED SUSPENSIONS

No.	Suspensions		Specific weight of deposition (mg/cm^2)	Effective percentile coverage of the films (%)	Surface quality of green films
	Solvent	% Vol.			
1	Ethanol	100	3.1	<20	-
2	Iso-propanol	100	No deposition	-	-
3	Ethanol + Acetone	25/75	2.1	<20	-
4	Ethanol + Acetone	50/50	2.7	<20	-
5	Ethanol + Acetone	75/25	6.5	□40-50	Uneven, incoherent with holes & cracks.
6	Iso-propanol+ Acetone	25/75	No deposition	-	-
7	Iso-propanol+ Acetone	50/50	No deposition	-	-
8	Iso-propanol+ Acetone	75/25	No deposition	-	-
9	THF + Acetone	25/75	10.1	□60-70	Uniform but rough with cracks.
10	THF + Acetone	50/50	8.7	□50-55	Uniform but rough with cracks.
11	THF + Acetone	75/25	11.6	□70-80	Uniform but rough with cracks.
12	Acetone	100	2.9	<20	-
13	**Tetrahydrofuran (THF)**	**100**	**16.32**	**□100**	**Uniform, smooth with cracks.**
14	Ethanol + Acetyl acetone	25/75	No deposition	-	-
15	Ethanol + Acetyl acetone	50/50	No deposition	-	-
16	Ethanol + Acetyl acetone	75/25	No deposition	-	-
17	Iso-propanol+ Acetyl acetone	25/75	No deposition	-	-
18	Iso-propanol+ Acetyl acetone	50/50	No deposition	-	-
19	Iso-propanol+ Acetyl acetone	75/25	No deposition	-	-
20	Ethanol + THF	25/75	12.5	□80-90	Uniform but rough with cracks.
21	Ethanol + THF	50/50	13.4	□85-90	Uniform but rough with cracks.
22	Ethanol + THF	75/25	14.2	□85-90	Uniform but rough with cracks.
23	Ethylene glycol	100	No deposition	-	-
24	Acetyl acetone	100	No deposition	-	-
25	Ethanol + Ethylene glycol	25/75	No deposition	-	-
26	Ethanol + Ethylene glycol	50/50	No deposition	-	-
27	Ethanol + Ethylene glycol	75/25	No deposition	-	-

28	Ethylene glycol + Acetone	25/75	No deposition	-	-
29	Ethylene glycol + Acetone	50/50	No deposition	-	-
30	Ethylene glycol+ Acetone	75/25	No deposition	-	-
31	THF + Acetyl acetone	25/75	11.3	□70-80	Uniform but rough with cracks.
32	THF + Acetyl acetone	50/50	12.2	□80-90	Uniform but rough with cracks.
33	THF + Acetyl acetone	75/25	13.6	□85-90	Uniform but rough with cracks.

Results and discussion

In order to identify the appropriate media for electrophoretic deposition of Bi_2Te_3 powders, a range of pure and mixed solvents were tested. The suspensions prepared are listed in Table 1.

The deposition weight per submerged area, specific weight, was measured for all of the tested suspensions (Table 1). The highest specific weight of deposition (16.32mg/cm^2) resulted in a Tetrahydrofuran (THF) suspension. Relatively high specific weights of deposition (8.7-14.2mg/cm^2) were also measured by mixing THF with other solvents such as Acetyl acetone and Ethanol, at various volume percentages. Although most of the suspensions resulted in no deposition, some of the suspensions showed a specific deposition weight below 3mg/cm^2, which is regarded as too low to produce coherent Bi_2Te_3 films as discussed later. In addition to the specific weight, the percentage of the submerged substrate area coated during 10 minutes' EPD deposition, the **effective percentile coverage**, was measured as a parameter to rank the effectiveness of the selected solvent and resulted suspension.

The effective percentile coverage (C) of the films was calculated using the following equation (3):

$$C(\%) = \frac{A_{film}}{A_{submerge}} * 100 \qquad (3)$$

Where A_{film} is the area of the substrate covered uniformly with the deposited film and $A_{submerge}$ is the total area of the substrate exposed to the suspension during the EPD process.

For A_{film} in Equation 3, SEM images from the entire surface area of the submerged substrate were examined closely to measure the coating area for every suspension precisely. The effective percentile coverage of all tested suspensions are given in Table 1. A perfect effective percentile coverage (100%) was achieved with the THF suspension (i.e. the entire submerged surface area of the substrate was coated evenly), followed by those suspensions containing THF in the media mixture (from 50-90%, Table 1).

The quality of deposited films was analyzed in a scanning electron microscope. The SEM micrographs along the inset images in Figure 2 confirm a better quality (homogenous with a smooth surface) for the films deposited from the THF suspension (Figure 2a). The films are coherent and have a uniform structure with no cracks or depressions visible under SEM. In addition, the thickness of the THF films was uniform and even (Figure 2b).

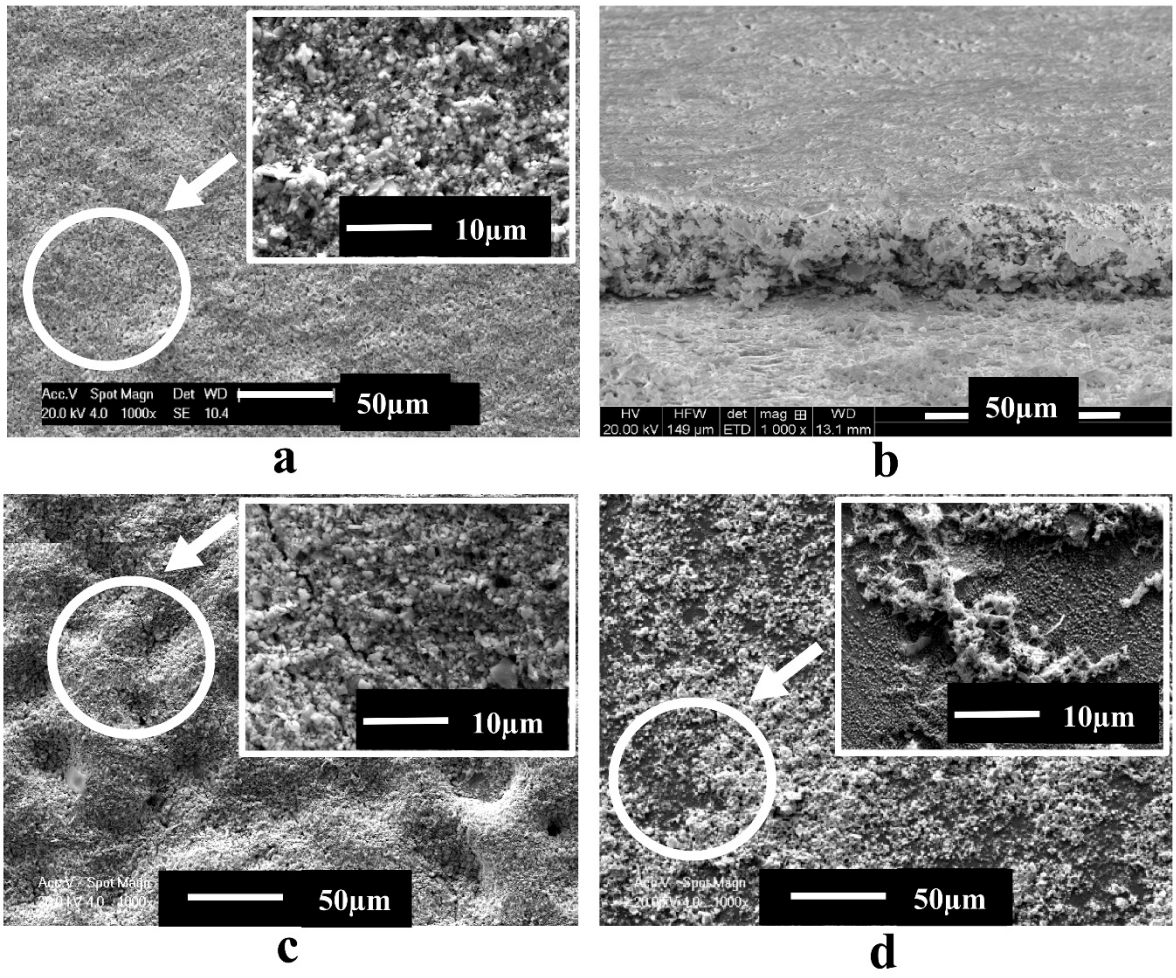

Figure 2. SEM micrographs of the green Bi_2Te_3 films to show the effect of the suspension type on the microstructure. (a and b) THF Suspension (No. 13) with uniform film thickness, (c) coatings with surface depressions and fine cracks, Suspension No. 22, (d) Inconsistent coatings, Suspension No. 5 (Table 1).

Conversely, the SEM images of the deposited films from other suspensions usually showed rough surfaces with cracks even in relatively high effective percentile coverages and high specific weights of depositions. This is clearly evident in Figure 2c and the inset on the top right highlights the formation of a fine crack for suspension No. 22. In addition, suspensions with low specific weights of depositions such as suspension No. 5 (Figure 2d) fail to form a consistent coating on the substrate; the coating does not cover the substrate uniformly.

The variation of the specific weights of deposition with the zeta potential measurements of the tested suspensions is plotted in Figure 3. The zeta potential of the particles in a suspension is one of the key factors in ensuring the deposition of optimal coating during the EPD process. It defines the electric potential in the interfacial double layer (DL) [20]. It determines the dispersion uniformity of the suspended particles, as well as the stability of the suspension [44]. The other parameter that governs a successful deposition is the particle mobility within the suspension. Electrophoretic mobility (EPM) is defined as the velocity of particles under the electric field [45]. The zeta potential and EPM are interconnected under EPD principles.

The SEM observation showed that only the two suspensions, No. 13 (THF) and 22 of Table 1, are of good quality with their zeta potential measurements falling within the 50-70 V range, Figure 3. This is in line with the DLVO (Derjaguin and Landau [46] and Verwey and Overbeek [47]) calculated optimal range of the zeta potential necessary to ensure good quality coating depositions via the EPD process. The accomplished uniform Bi_2Te_3 films from THF suspensions with the optimal zeta potential range have the highest effective percentile coverages and deposition rates as well (Table 1).

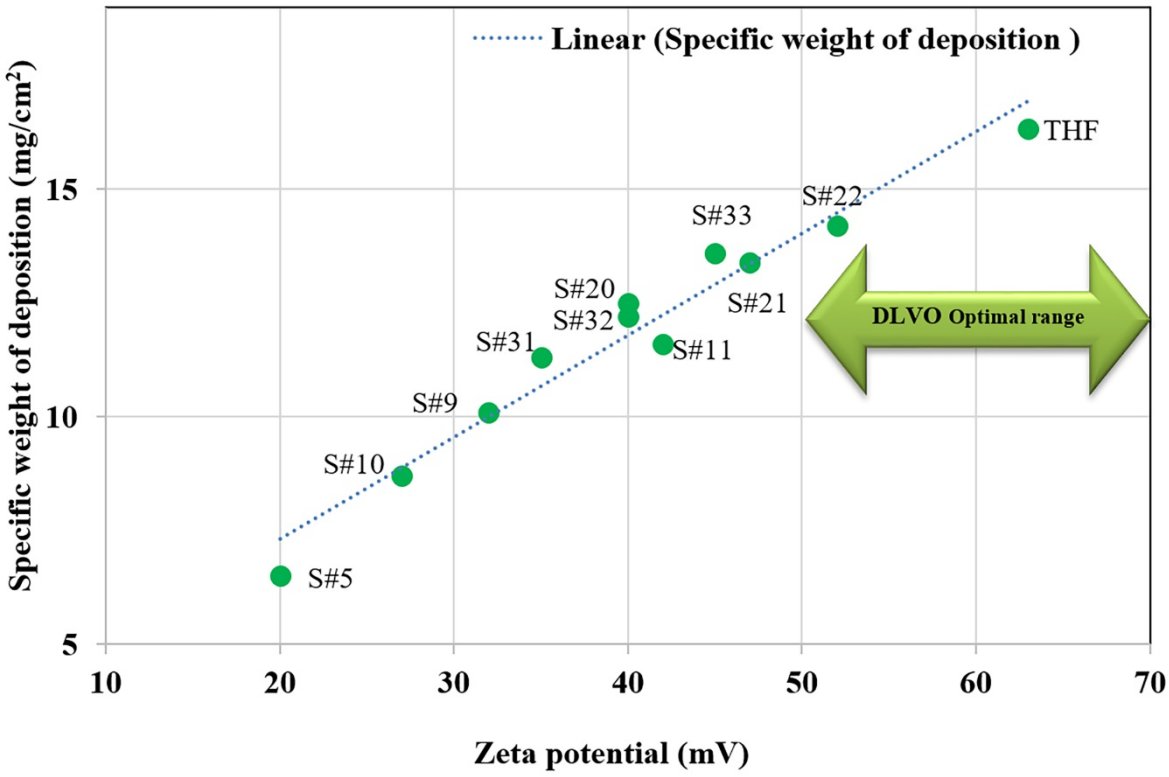

Figure 3. Variations of specific weights of depositions with the zeta potentials of the particles for different suspension compositions.

In DLVO theory, the forces between the charged particles interacting through a liquid medium were calculated [48]. DLVO theory points out that the dominant interparticle forces in a colloidal suspension are the van der Waals attractive forces and the electrostatic and steric repulsive forces from the double layer and polymeric solubilizers, respectively. Hence, to achieve a stable suspension, a high deposition yield and a highly uniform film, the existence of a sufficient repulsive force from the double layer, i.e. the zeta potential, combined with a well-balanced van der Waals attractive force, is necessary [20, 49]. In addition, an adequate zeta potential and EPM values lead to high green density by creating a powerful repulsive force between the particles when occupying positions in the deposition [20, 24, 34, 35, 45, 50]. Therefore, it

was calculated that there is an ideal range of the zeta potential (50-70mV) to have an effective EPD process [20, 51].

These conditions are essential to have particles with high electrophoretic mobility under the electric field, which can lead to a successful EPD process [48, 51]. Basically, the amount of electrophoretic mobility shows the velocity of particles under the electric field [20]. Therefore, in theory, as Equations 1 and 2 suggest, a higher electrophoretic mobility should lead to a higher specific weight of deposition, which is confirmed clearly by the experimental results (Figure 4).

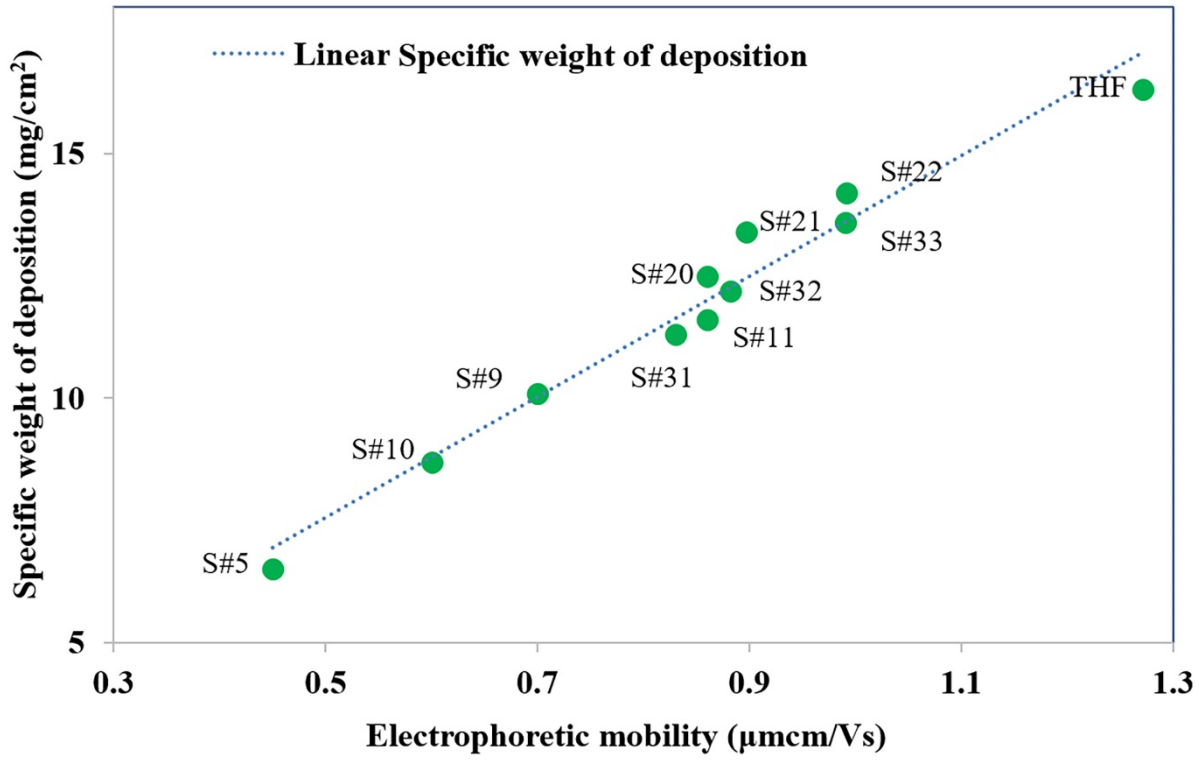

Figure 4. Variations of specific weights of depositions with the electrophoretic mobilities of the particles for different suspension compositions.

On the contrary, the suspensions with less ideal zeta potentials resulted in lower specific weights of depositions (Figure 3) as well as lower effective percentile coverages (Table 1). The results are in good agreement with EPD theoretical principles because, according to Hamaker's equations, (Equations 1 and 2), the zeta potential and electrophoretic mobility have a direct, dependent relationship with the specific deposition weights [34, 52]. These relationships were also confirmed by the experimental results (Figure 4), which show a similar trend for the specific deposition weights to the ones of zeta potential and electrophoretic mobility [20, 24, 34, 35, 45, 50].

Furthermore, measuring the electrical conductivity of the suspensions is a useful means to investigate the behaviour of ions and the charged particles of suspensions in the EPD process. The conductivity shows important interactions between the solvent, the powder and free ions included in the charge transfer. It also indicates the ionic strength of the solvent.

The conductivity of the THF suspensions rose gently with an increase in the second solvent concentration (Figure 5). However, at the same time, the specific weight of deposition decreased in a similar manner. Comparable trends were observed for the suspensions conductivity and the specific weights of depositions for ethanol, acetone and acetyl acetone suspensions, changing from 2.2μS/cm for pure THF to 5.8-6.2μS/cm for the highest concentrations in different suspensions. The mixture of ethanol and acetone showed the maximum conductivity where it yielded the lowest specific deposition weight (Figure 5).

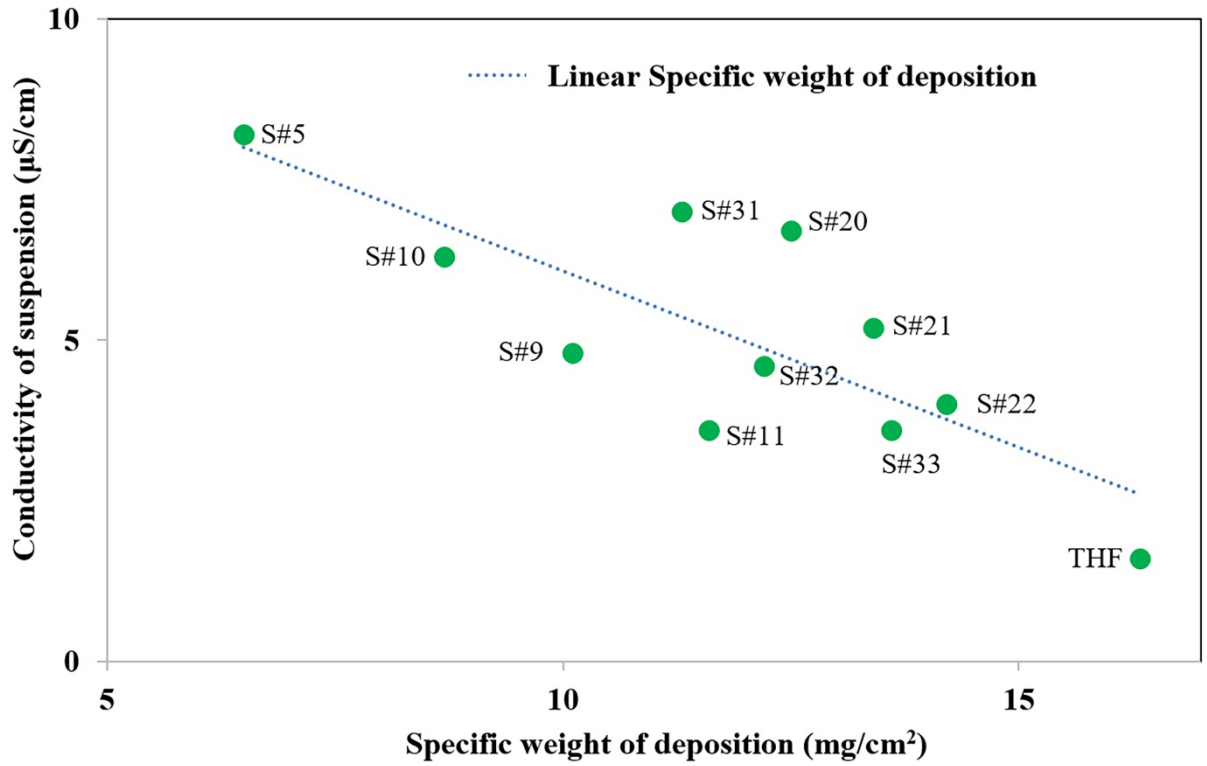

Figure 5. Variations of specific weights of depositions with the conductivities of the suspensions for the different suspension compositions.

One explanation that has been suggested to describe this phenomenon is that, since the suspension conductivity is a measure of the ratio between the H^+ ions and the charged particles, the higher conductivities (such as in the ethanol and acetone mixture) indicate a higher fraction of ions and therefore a lower fraction of charged particles in the suspension, which leads to a lower deposition yield [53]. That is why other studies have also chosen suspensions with lower conductivity when comparing suspensions and determining the best ones for various applications [39].

Another explanation could be attributed to the concentration of free ions. A high free ion concentration may hinder the movement of particles by decreasing the effective current of the EPD process on the particles by transferring a large portion of the current between the

electrodes [54]. In addition, it was proposed that in a "too conductive" suspension, particle motion is very limited [20, 52, 53]. Conversely, if the resistivity of the suspension is too high, achieving a stable suspension with adequately charged particles is difficult [55, 56]. Therefore, the electrophoretic deposition is feasible in a narrow band of the conductivity range [44, 48]. In addition, this suitable region varies for different systems of materials and media [20, 34].

To characterize the thermoelectric properties of the deposited films, the in-plane Seebeck coefficients of deposited films were measured at room temperature (300K) after sintering at 693K for 1 hour. To confirm the stoichiometry of the green and sintered films, XRD analysis of the films was performed (Figure 6) and the existence of the *p*-type Bi_2Te_3 phase is confirmed. No other phases and no changes were identified because of the sintering process. All peaks could be assigned to the rhombohedral structure, as previously reported [57-59]. The peaks exactly correspond to the (006), (015), (1010), (0111), (0015) and (115) reflections of the $Bi_{0.5}Se_{1.5}Te_3$ compound in the stable Bi_2Te_3 phase [57-59]. In addition, the chemical composition and weight percentages of *p*-type Bi_2Te_3 powder were measured using the EDX (Energy-dispersive X-ray spectroscopy) of SEM [19] and its chemical formula was calculated as $Bi_{0.5}Se_{1.5}Te_3$.

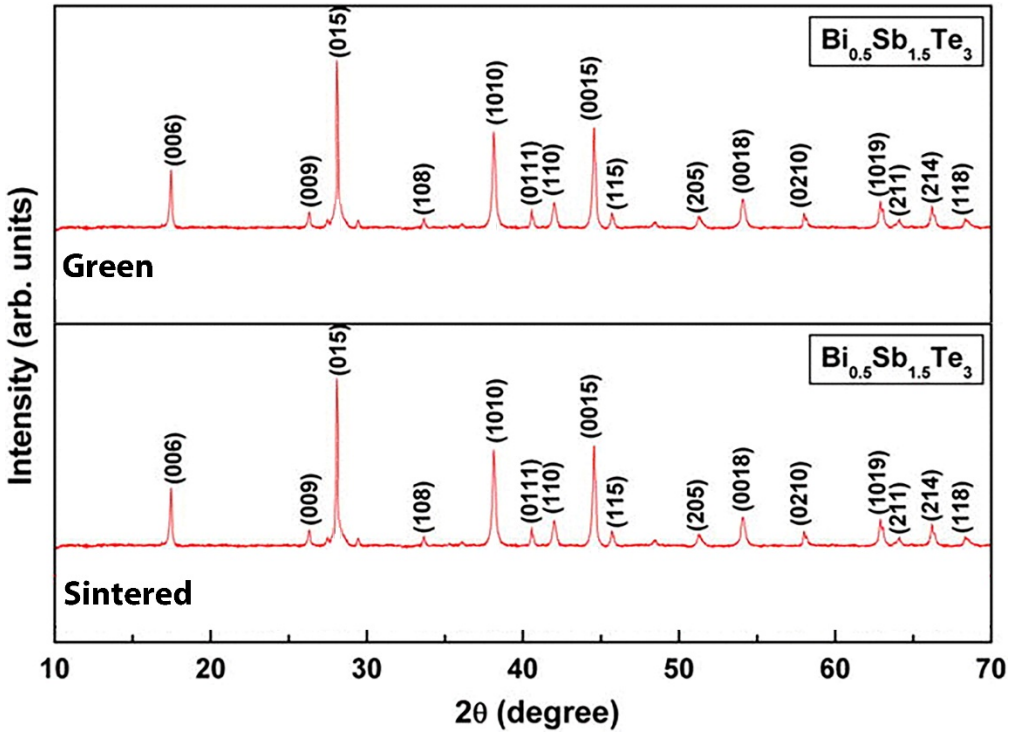

Figure 6. XRD results of (a) green and (b) sintered *p*-type Bi_2Te_3 films.

The results show that the Seebeck coefficients had a positive value, as expected, because a *p*-type Bi_2Te_3 powder was used to deposit the films (Figure 7). The Seebeck coefficients of the films deposited from the THF suspensions (126 μV/K) were approximately 20% higher than the Seebeck coefficients of the films deposited from the next best suspension (No. 22) (100 μV/K). In addition, the Seebeck coefficients of the films decreased with the reduction in the specific weight of depositions and effective percentile coverage in various suspensions (Figure 6 and Table 1). It is also clear that the Seebeck coefficients of the films deposited from suspension No. 5 (58 μV/K) were less than half that of the THF suspensions (126 μV/K). The reasons for the better thermoelectric performance may include the higher densities and specific weights of depositions of the films deposited from the suspensions with higher zeta potential (THF and No. 22). The density of these films was 7.04 and 6.93 g/cm^3 respectively,

which is approximately 90% of the theoretical density of Bi_2Te_3 powder (7.74 g/cm^3). While the densities of the film deposited from some of the suspensions with 60-70% effective percentile coverage, such as No. 9, were much lower, at about 5.39 g/cm^3. Higher film density can contribute to the charge carrier diffusion [1, 3, 6], phonon drag [60-62] of a material and, consequently, an increase in the Seebeck coefficient and thermoelectric properties [3, 6, 62, 63].

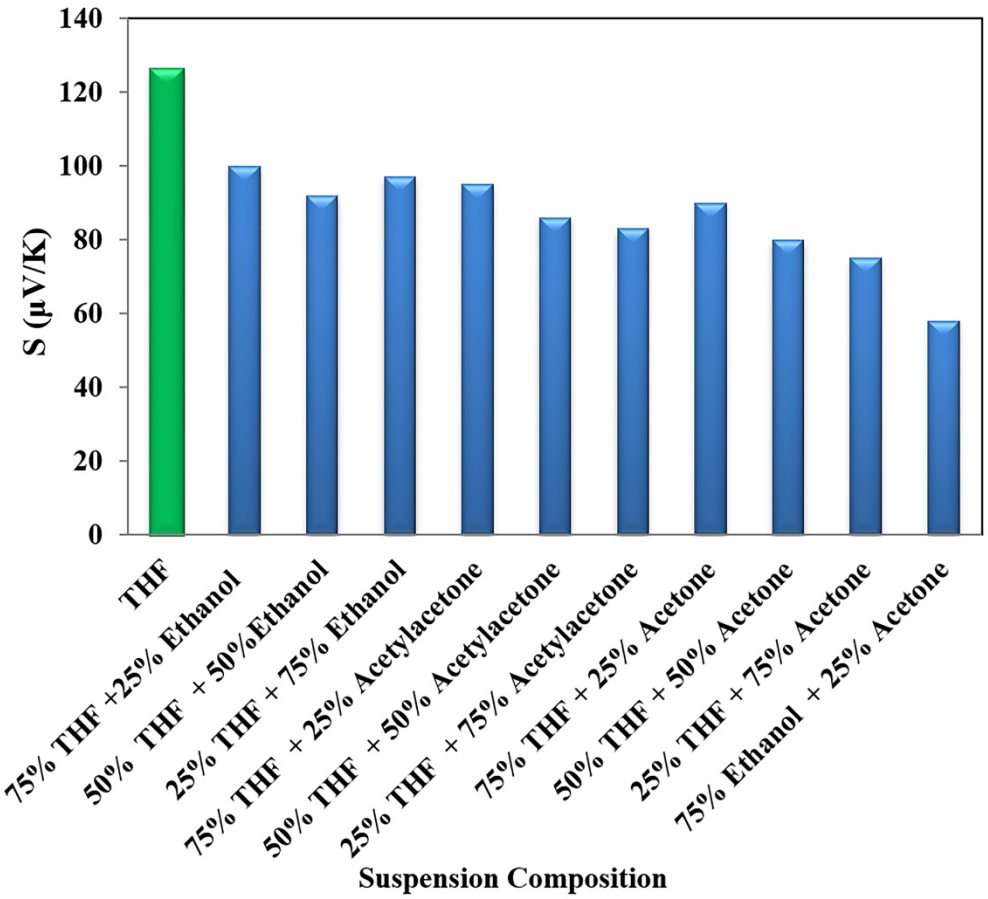

Figure 7. Variations of the Seebeck coefficients with the Suspension Compositions at room temperature. (All percentages are by volume.)

Different values of in-plane Seebeck coefficients were reported by researchers using various deposition methods to prepare a Bi_2Te_3 film. Comparing the thermoelectric properties of the Bi_2Te_3 films prepared using the EPD method (126 μV/K) with similar methods such as the

electrodeposition technique [13] (80 μV/K), shows a 50% improvement in thermoelectric performance when using the EPD method. This improvement may be due to unwanted elements of the solutions, such as chlorine, that are omitted from the films using the electrodeposition technique, as well as the higher film density offered by the EPD method (around 90% from EPD and 80% from electrodeposition) [13].

Furthermore, an in-plane Seebeck coefficient of 160 μV/K at 300 K was measured when a co-sputtering method was used to deposit a Bi_2Te_3 film [9]. In comparison with the EPD method (126 μV/K at 300 K), the co-sputtering method is a complex process and requires expensive equipment to reach only a relatively higher Seebeck coefficient. Furthermore, the co-sputtering process is slow (with a deposition rate of 0.03μm per minute) and needs good vacuum pressure (6.0×10^{-4} Pa). During the EPD process, there is no need to have a vacuum chamber or any expensive equipment and the deposition rate is much higher (with a deposition rate of more than 2μm per minute, or approximately 60 times faster). Although the first recorded Seebeck coefficient is around 25% lower, the finished cost is much lower, which makes EPD a more attractive option for commercial TE applications. Beyond this, the Seebeck coefficient of the films deposited by EPD can be improved by increasing the film density and other methods such as doping, which will be reported in future publications.

Conclusions

In summary, a coherent crack-free *p*-type Bi_2Te_3 film was fabricated successfully using an electrophoretic deposition for thermoelectric applications. After a thorough investigation of various suspensions, it was revealed that the THF suspensions resulted in the highest specific weights of deposition and entire effective percentile coverage of the substrates. In addition, the SEM images showed highly uniform structures and thicknesses of the films deposited

from THF suspensions. The outcomes of this work show that the media and the electrical conductivity of the suspensions, as well as the zeta potential of the particles, play important roles in the EPD process. Furthermore, the in-plane Seebeck coefficients of the EDP prepared Bi_2Te_3 films were better than some of the other more expensive and complex film deposition methods. Its efficiency is comparable with some of the most expensive film fabrication techniques.

Acknowledgments

This work has been supported by the Australian Government Research Training Program Scholarship and The University of Adelaide. Financial support from Adelaide University under DVC(R) Research Equipment & Infrastructure award-2015 is also gratefully acknowledged.

References

1. G. S. Nolas, J. Poon, and M. Kanatzidis, *MRS Bulletin,* **31** (03), 199-205 (2006).
2. M. S. Dresselhaus, G. Chen, M. Y. Tang, R. G. Yang, H. Lee, D. Z. Wang, Z. F. Ren, J. P. Fleurial, and P. Gogna, *Advanced Materials,* **19** (8), 1043-1053 (2007).
3. M. Hamid Elsheikh, D. A. Shnawah, M. F. M. Sabri, S. B. M. Said, M. Haji Hassan, M. B. Ali Bashir, and M. Mohamad, *Renewable and Sustainable Energy Reviews,* **30** 337-355 (2014).
4. A. Zhou, Q. Fu, W. Zhang, B. Yang, J. Li, P. Ziolkowski, E. Mueller, and D. Xu, *Electrochimica Acta,* **178** 217-224 (2015).
5. X. Liu, W.-y. Zhao, H.-y. Zhou, X. Mu, D.-q. He, W.-t. Zhu, P. Wei, H. Wu, and Q.-j. Zhang, *Journal of Electronic Materials,* **45** (3), 1328-1335 (2015).
6. H. Alam and S. Ramakrishna, *Nano Energy,* **2** (2), 190-212 (2013).
7. H. Scherrer and S. Scherrer. CRC Press, Boca Raton, 2006.
8. K. Wojciechowski, E. Godlewska, K. Mars, R. Mania, G. Karpinski, P. Ziolkowski, C. Stiewe, and E. Müller, *Vacuum,* **82** (10), 1003-1006 (2008).
9. Z.-k. Cai, P. Fan, Z.-h. Zheng, P.-j. Liu, T.-b. Chen, X.-m. Cai, J.-t. Luo, G.-x. Liang, and D.-p. Zhang, *Applied Surface Science,* **280** 225-228 (2013).
10. H.-J. Lee, H. S. Park, S. Han, and J. Y. Kim, *Thermochimica Acta,* **542** 57-61 (2012).
11. Z. Zeng, P. Yang, and Z. Hu, *Applied Surface Science,* **268** 472-476 (2013).
12. X. Wang, H. He, N. Wang, and L. Miao, *Applied Surface Science,* **276** 539-542 (2013).
13. C. Lei, K. S. Ryder, E. Koukharenko, M. Burton, and I. S. Nandhakumar, *Electrochemistry Communications,* **66** 1-4 (2016).
14. J. Dheepa, R. Sathyamoorthy, and S. Velumani, *Materials Characterization,* **58** (8–9), 782-785 (2007).

15. C. Raub, in *Metal Plating and Patination*, p. 284-290, Butterworth-Heinemann, (1993).
16. R. Child, in *Metal Plating and Patination*, p. 291-300, Butterworth-Heinemann, (1993).
17. J. H. We, S. J. Kim, G. S. Kim, and B. J. Cho, *Journal of Alloys and Compounds,* **552** 107-110 (2013).
18. T. Talebi, R. Ghomashchi, P. Talemi, and S. Aminorroaya, *International Journal of Chemical, Molecular, Nuclear, Materials and Metallurgical Engineering,* **11** (4), 11 - 14 (2017).
19. T. Talebi, R. Ghomashchi, P. Talemi, and S. Aminorroaya, *International Journal of Chemical, Molecular, Nuclear, Materials and Metallurgical Engineering,* **11** (4), (2017).
20. L. Besra and M. Liu, *Progress in Materials Science,* **52** (1), 1-61 (2007).
21. A. R. Boccaccini and I. Zhitomirsky, *Current Opinion in Solid State and Materials Science,* **6** (3), 251-260 (2002).
22. K. Hayashi and N. Furuya, *Journal of The Electrochemical Society,* **151** (3), A354-A357 (2004).
23. M. Diba, D. W. H. Fam, A. R. Boccaccini, and M. S. P. Shaffer, *Progress in Materials Science,* **82** 83-117 (2016).
24. C. P. Gutierrez, J. R. Mosley, and T. C. Wallace, *Journal of The Electrochemical Society,* **109** (10), 923-927 (1962).
25. M. S. Ata and I. Zhitomirsky, *Advances in Applied Ceramics: Structural, Functional & Bioceramics,* **111** (5/6), 345-350 (2012).
26. K. Hasegawa, S. Kunugi, M. Tatsumisago, and T. Minami, *Journal of Sol-Gel Science and Technology,* **15** (3), 243-249 (1999).
27. M. Wei, A. J. Ruys, B. K. Milthorpe, C. C. Sorrell, and J. H. Evans, *Journal of Sol-Gel Science and Technology,* **21** (1), 39-48 (2001).
28. W. Shan, Y. Zhang, W. Yang, C. Ke, Z. Gao, Y. Ye, and Y. Tang, *Microporous and Mesoporous Materials,* **69** (1–2), 35-42 (2004).
29. A. R. Boccaccini, J. Cho, T. Subhani, C. Kaya, and F. Kaya, *Journal of the European Ceramic Society,* **30** (5), 1115-1129 (2010).
30. S. J. Limmer and G. Cao, *Advanced Materials,* **15** (5), 427-431 (2003).
31. M. J. Shane, J. B. Talbot, B. G. Kinney, E. Sluzky, and K. R. Hesse, *Journal of Colloid and Interface Science,* **165** (2), 334-340 (1994).
32. J. Van Tassel and C. A. Randall, *Journal of the European Ceramic Society,* **19** (6–7), 955-958 (1999).
33. S. Put, J. Vleugels, G. Anné, and O. Van der Biest, *Colloids and Surfaces A: Physicochemical and Engineering Aspects,* **222** (1–3), 223-232 (2003).
34. H. C. Hamaker, *Transactions of the Faraday Society,* **35** (0), 279-287 (1940).
35. P. Sarkar and P. S. Nicholson, *Journal of the American Ceramic Society,* **79** (8), 1987-2002 (1996).
36. R. N. Basu, C. A. Randall, and M. J. Mayo, *Journal of the American Ceramic Society,* **84** (1), 33-40 (2001).
37. M. A. Islam, Y. Xia, D. A. Telesca, M. L. Steigerwald, and I. P. Herman, *Chemistry of Materials,* **16** (1), 49-54 (2004).
38. T. Talebi, B. Raissi, and A. Maghsoudipour, *International Journal of Hydrogen Energy,* **35** (17), 9434-9439 (2010).
39. B. R. I. A. Borojeni, A. Maghsoudipour, M. Kazemzad, E. Marzbanrad,, *Key Engineering Materials,* **412** 279-285 (2009).
40. H. Sa'adati, B. Raissi, R. Riahifar, and M. S. Yaghmaee, *Journal of the European Ceramic Society,* **36** (2), 299-305 (2016).
41. S. V. Mahajan and J. H. Dickerson, *Nanotechnology,* **21** (14), 145704 (2010).
42. P. H. Janet Hope, *Key Engineering Materials,* **507** 175-179 (2012).
43. G. Anné, K. Vanmeensel, J. Vleugels, and O. Van der Biest, *Colloids and Surfaces A: Physicochemical and Engineering Aspects,* **245** (1–3), 35-39 (2004).

44. L. Stappers, L. Zhang, O. Van der Biest, and J. Fransaer, *Journal of Colloid and Interface Science,* **328** (2), 436-446 (2008).
45. O. O. V. d. B. and and L. J. Vandeperre, *Annual Review of Materials Science,* **29** (1), 327-352 (1999).
46. B. Derjaguin and L. Landau, *Progress in Surface Science,* **43** (1), 30-59 (1993).
47. E. J. W. Verwey, *The Journal of Physical and Colloid Chemistry,* **51** (3), 631-636 (1947).
48. D. Horinek, in *Encyclopedia of Applied Electrochemistry*, G. Kreysa, K.-i. Ota and R. F. Savinell, eds., p. 343-346, Springer New York, New York, NY, (2014).
49. B. V. Derjaguin, T. N. Voropayeva, B. N. Kabanov, and A. S. Titiyevskaya, *Progress in Surface Science,* **43** (1), 83-105 (1993).
50. I. Corni, M. P. Ryan, and A. R. Boccaccini, *Journal of the European Ceramic Society,* **28** (7), 1353-1367 (2008).
51. B. Ferrari and R. Moreno, *Journal of the European Ceramic Society,* **30** (5), 1069-1078 (2010).
52. H. C. Hamaker, *Physica,* **4** (10), 1058-1072 (1937).
53. S. Dor, S. Rühle, A. Ofir, M. Adler, L. Grinis, and A. Zaban, *Colloids and Surfaces A: Physicochemical and Engineering Aspects,* **342** (1–3), 70-75 (2009).
54. K. Moritz and E. Müller, *Journal of Materials Science,* **41** (24), 8047-8058 (2006).
55. B. Ferrari and R. Moreno, *Journal of the European Ceramic Society,* **17** (4), 549-556 (1997).
56. B. Ferrari and R. Moreno, *Materials Letters,* **28** (4), 353-355 (1996).
57. X. Yan, B. Poudel, Y. Ma, W. S. Liu, G. Joshi, H. Wang, Y. Lan, D. Wang, G. Chen, and Z. F. Ren, *Nano Letters,* **10** (9), 3373-3378 (2010).
58. H. Goldsmid, *Materials,* **7** (4), 2577 (2014).
59. S.-j. Jeon, H. Jeon, S. Na, S. D. Kang, H.-K. Lyeo, S. Hyun, and H.-J. Lee, *Journal of Alloys and Compounds,* **553** 343-349 (2013).
60. A. M. Rao, X. Ji, and T. M. Tritt, *MRS Bulletin,* **31** (03), 218-223 (2006).
61. W. Liu, X. Yan, G. Chen, and Z. Ren, *Nano Energy,* **1** (1), 42-56 (2012).
62. A. Shakouri, *Annual Review of Materials Research,* **41** (1), 399-431 (2011).
63. G. Schierning, *physica status solidi (a),* **211** (6), 1235-1249 (2014).